Steel and Composite Structures, *Vol. 17, No. 2 (2014) 173-184*
DOI: http://dx.doi.org/10.12989/scs.2014.17.2.173

Research on residual stress in SiC_f reinforced titanium matrix composites

Haitao Qu [1a], Hongliang Hou [*1], Bing Zhao [1b] and Song Lin [2c]

[1] *Beijing Aeronautical Manufacturing Technology Research Institute, Beijing 100024, China*
[2] *Shijiazhuang Tiedao University, Shijiazhuang 050043, China*

(*Received February 21, 2014, Revised May 30, 2014, Accepted June 24, 2014*)

Abstract. This study aimed to theoretical calculate the thermal residual stress in continuous SiC fiber reinforced titanium matrix composites. The analytical solution of residual stress field distribution was obtained by using coaxial cylinder model, and the numerical solution was obtained by using finite element model (FEM). Both of the above models were compared and the thermal residual stress was analyzed in the axial, hoop, radial direction. The results indicated that both the two models were feasible to theoretical calculate the thermal residual stress in continuous SiC fiber reinforced titanium matrix composites, because the deviations between the theoretical calculation results and the test results were less than 8%. In the titanium matrix composites, along with the increment of the SiC fiber volume fraction, the longitudinal property was improved, while the equivalent residual stress was not significantly changed, keeping the intensity around 600 MPa. There was a pronounced reduction of the radial residual stress in the titanium matrix composites when there was carbon coating on the surface of the SiC fiber, because carbon coating could effectively reduce the coefficient of thermal expansion mismatch between the fiber and the titanium matrix, meanwhile, the consumption of carbon coating could protect SiC fibers effectively, so as to ensure the high-performance of the composites. The support of design and optimization of composites was provided though theoretical calculation and analysis of residual stress.

Keywords: titanium matrix composites; thermal residual stress; coaxial cylinder model; finite element model; theoretical calculation

1. Introduction

With the rapid development of aviation industry, high-thrust-weight ratio aeroengine has become a research focus. Vassel (1999) and Feillard (1996) had studied the greater performance of the continuous SiC fiber reinforced titanium matrix composites compared with the traditional titanium alloy material. According to the publications (Lou *et al*. 2010, Gundel and Warrier 1996, Gundel *et al*. 1999, Subramanian *et al*. 1998, Wood and Close 1995, Fukushima *et al*. 2000, Thomas and Winstone 1999), it was shown that the continuous SiC fiber reinforced titanium

*Corresponding author, Professor, E-mail: applelisx@126.com
[a] Ph.D., E-mail: quhaitao526@126.com
[b] Ph.D., E-mail: zhao6833@163.com
[c] Master Student, E-mail: 327610339@qq.com

http://www.techno-press.org/?journal=scs&subpage=8 ISSN: 1229-9367 (Print), 1598-6233 (Online)

matrix composites had become the most promising structural material because of its high temperature properties and high specific strength combined stiffness.

Thermal residual stress was usually brought in during the cooling process when continuous SiC fiber reinforced titanium matrix composites were fabricated, because the coefficient of thermal expansion mismatch between the fiber and the titanium matrix. The presence of residual stress had great influence on the performance of the composites. It was described that the tensile strength of the composites could be enhanced when there was longitudinal residual compressive stress in the fibers and cracks could be introduced when there was transverse residual tensile stress in the matrix by Arsenault and Taya (1987). The publications (Majumdar 1999, Qu *et al*. 2011) showed that the coating on the SiC fiber could influence thermal residual stress. Therefore, it was necessary to analyze thermal residual stress for design and optimization of components in the continuous SiC fiber reinforced titanium matrix composites.

2. Experimental methods

There were two methods of the residual stress analysis at present: experimental measurement and theoretical calculation. It had been difficult to measure the residual stress by experiment which led to obvious deviation. The result of X-ray diffraction had strong randomicity and corresponding penetration depth was only 10 μm (Oddershede *et al*. 2010). Although the penetration depth was increased by neutron diffraction, corresponding test cost was high (Woo *et al*. 2011). The titanium matrix needed to be peeled off which led to the change of the stress state when using Raman spectroscopy and the accuracy of the results cannot be guaranteed (Mao *et al*. 2010).

As mentioned above, all the experimental measurements were aimed at calculating the average residual stress of some region of the composite material. At present, distribution of residual stresses in the whole material, especially at the interface, could only be showed through theoretical calculation which included analytical method and numerical method.

Continuous coaxial cylinder model was commonly used when using analytical method to calculate residual stress in SiC fiber reinforced titanium matrix composites. The model was established by Mikata and Taya (1985) and amended by Warwick and Clyne (1991). It could be used to calculate residual stress of the fiber reinforced titanium matrix composites with N components.

The numerical method usually analyzed the residual stress distribution through the finite element software Abaqus (Ma *et al*. 2004, Huang *et al*. 2009, Warrier *et al*. 1999).

3. Continuous coaxial cylinder model

Continuous SiC fiber reinforced titanium matrix composites were transversely isotropiccmedia. When the temperature was changed, the analytic solutions of elastic stress state exsisted. Thus, the residual stress and its distribution in the composites could be calculated by the continuous coaxial cylinder model.

When there was 3 components, that was $N = 3$, the established continuous coaxial cylinder model was showed in Fig. 1. Based on the stress equilibrium relationship in the model, Eq. (1) showed the relational expressions of the nine stress components under the cylindrical coordinates systems.

$$\frac{1}{r}\frac{\partial}{\partial r}\left(r\sigma_{rr}^{(n)}\right)+\frac{1}{r}\frac{\partial\sigma_{r\theta}^{(n)}}{\partial\theta}+\frac{\partial\sigma_{rz}^{(n)}}{\partial z}-\frac{\partial\sigma_{\theta\theta}^{(n)}}{r}=0$$

$$\frac{1}{r}\frac{\partial}{\partial r}\left(r^2\sigma_{\theta r}^{(n)}\right)+\frac{1}{r}\frac{\partial\sigma_{\theta\theta}^{(n)}}{\partial\theta}+\frac{\partial\sigma_{\theta z}^{(n)}}{\partial z}=0 \tag{1}$$

$$\frac{1}{r}\frac{\partial}{\partial r}\left(r\sigma_{zr}^{(n)}\right)+\frac{1}{r}\frac{\partial\sigma_{z\theta}^{(n)}}{\partial\theta}+\frac{\partial\sigma_{zz}^{(n)}}{\partial z}=0$$

According to the relationship between the stress, strain and displacement, solutions of Eq. (1) could be expressed as

$$\sigma_{rr}=C_{11}^{(n)}\left[A_n-\frac{B_n}{r^2}\right]+C_{12}^{(n)}\left[A_n-\frac{B_n}{r^2}\right]+C_{13}^{(n)}E-\beta_1^{(n)}\Delta T$$

$$\sigma_{\theta\theta}=C_{11}^{(n)}\left[A_n-\frac{B_n}{r^2}\right]+C_{12}^{(n)}\left[A_n-\frac{B_n}{r^2}\right]+C_{13}^{(n)}E-\beta_1^{(n)}\Delta T \tag{2}$$

$$\sigma_{zz}=2C_{13}^{(n)}A_n+C_{33}^{(n)}E-\beta_3^{(n)}\Delta T$$

$$\sigma_{rz}=\sigma_{\theta z}=\sigma_{r\theta}=0$$

Where n represented number of the coaxial cylinder layers; A, B and E were integral constants.

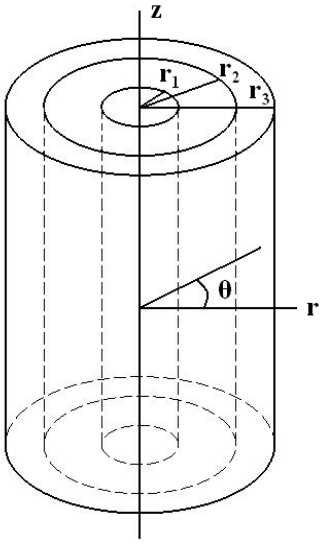

Fig. 1 The continuous coaxial cylinder model

$$\beta_1^{(n)} = \left(C_{11}^{(n)} + C_{12}^{(n)}\right)\alpha^{(n)} + C_{13}^{(n)}\alpha^{(n)};$$

$$\beta_3^{(n)} = 2C_{12}^{(n)}\alpha^{(n)} + C_{33}^{(n)}\alpha^{(n)};$$

$$C_{11} = C_{33} = \frac{E_i(1-v^2)}{k};$$

$$C_{12} = C_{13} = \frac{E_i v(1+v)}{k}$$

$$C_{44} = G_L = \frac{E_i}{2(1+v)}.$$

Considering the boundary conditions of continuous coaxial cylinder:

(1) Radial stress on the outer surface of the coaxial cylinder equaled to zero

$$A_N\left[C_{11}^{(N)} + C_{12}^{(N)}\right] + B_N\left[\frac{C_{12}^{(N)} - C_{11}^{(N)}}{r_N^2}\right] + EC_{13}^{(N)} - \beta_1^{(N)}\Delta T = 0 \tag{3}$$

(2) Moment equilibrium

$$\sum_{n=1}^{N}\int_{r_{n-1}}^{r_n}\sigma_{zz}^{(n)} r dr = \sum_{i=1}^{N}\left[2C_{13}^{(i)}A_i + C_{33}^{(i)}E - \beta_3^{(i)}\Delta T\right]\left(r_i^2 - r_{i-1}^2\right) = 0 \tag{4}$$

(3) Outer surface of layer i and inerter surface of layer i+1 had the same stress state

$$A_k r_k - A_{k+1}r_k + \frac{B_k}{r_k} - \frac{B_{k+1}}{r_k} = 0 \tag{5}$$

$$A_k r_k - A_{k+1}r_k + \frac{B_k}{r_k} - \frac{B_{k+1}}{r_k} = 0 \quad \left(k = 1 \text{ to } N-1\right) \tag{6}$$

$$\begin{aligned} &A_i\left[C_{11}^{(i)} + C_{12}^{(i)}\right] - A_{i+1}\left[C_{11}^{(i+1)} + C_{12}^{(i+1)}\right] + B_i\left[\frac{C_{12}^{(i)} - C_{11}^{(i)}}{r_i^2}\right] - \beta_{1+1}\left[\frac{C_{12}^{(i+1)} - C_{11}^{(i+1)}}{r_{i+1}^2}\right] \\ &+ E\left[C_{13}^{(i)} - C_{13}^{(i+1)}\right] = \Delta T\left(\beta_1^{(i)} - \beta_1^{(i+1)}\right) \end{aligned} \tag{7}$$

2N equations were built and then combined together, Eq. (8) could be obtained.

$$\begin{matrix} b_1 & b_2 & \cdots & b_{2N-1} & b_{2N} \end{matrix} = \begin{pmatrix} a_{1,1} & a_{1,2} & \cdots & a_{1,2N-1} & a_{1,2N} \\ a_{2,1} & \cdots & \cdots & \cdots & a_{1,2N} \\ \vdots & \vdots & \vdots & \vdots & \vdots \\ a_{2N-1,1} & \cdots & \cdots & \cdots & a_{2N-1,2N} \\ a_{2N,1} & \cdots & \cdots & \cdots & a_{2N,2N} \end{pmatrix} \begin{pmatrix} A_1 \\ \vdots \\ A_N \\ B_2 \\ \vdots \\ B_N \\ E \end{pmatrix} \tag{8}$$

a_i and b_i could be obtained according to Eqs. (3)-(8). Substituting them into Eq. (8), A, B, E could be calculated, and then following Eq. (2), σ_{rr}, $\sigma_{\theta\theta}$, σ_{zz} could be obtained, that was the distribution of residual stress in continuous coaxial cylinder model.

4. Finite element model

The finite element software Abaqus was used in this work. As shown in Fig. 2, the unit was 3D-single fiber model. The fiber diameter was 100 μm and the thickness along the fiber's length was 1 μm. The titanium layer with a thickness of 35 μm deposited on the SiC fiber by physical vapor deposition.

In the model, $x = 0$, $y = 0$, $z = 0$ were all symmetry plane. The nodes at $x = 85$ μm, $y = 85$ μm and $z = 1$ μm were coupled to displace equally in the x, y and z directions, respectively. The interface between the SiC fiber and the titanium matrix was assumed to be perfectly bonded. Table 1 showed the performance parameters of titanium alloy, SiC fiber and C coating.

The stress-free temperature was the key point to analyze the residual stress distribution for the continuous SiC fiber reinforced titanium matrix composites. During the cooling process after fabricated to the stress-free temperature, thermal residual stress was negligible due to the effect of high temperature creep. When cooled the composites from stress-free temperature to room

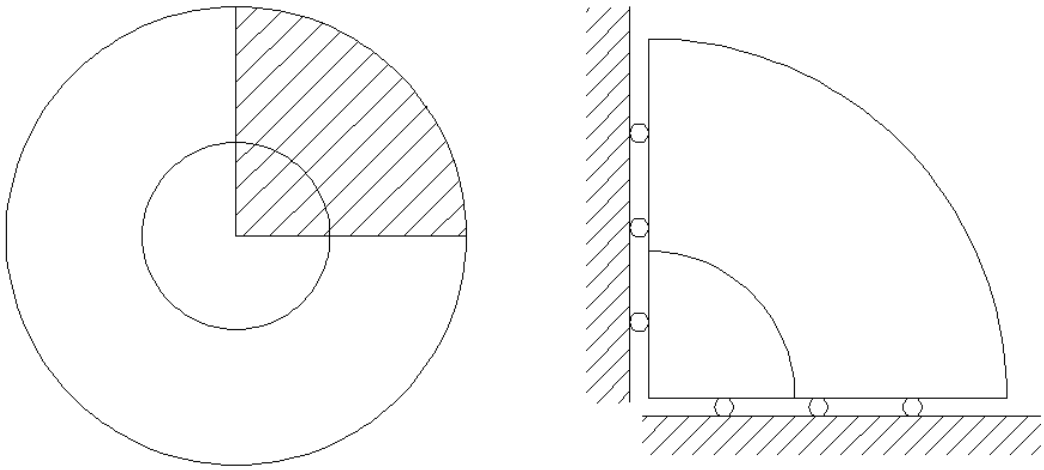

Fig. 2 The finite element model

Table 1 Performance parameters of titanium alloy, SiC fiber and C coating

Performance parameters	SiC fiber	C coating	Titanium alloy
Elastic modulus (GPa)	420	25	115
Shear modulus (GPa)	180	10	43
Poisson ratio	0.17	0.23	0.36
Coefficient*	4.0	7	9.0

*Coefficient: Coefficient of thermal expansion ($10^{-6}\cdot K^{-1}$)

temperature, the matrix shared heat load with fiber and thermal residual stress was brought in due to the coefficient of thermal expansion mismatch between the fiber and matrix.

Warrier *et al*. (1999) reported that the stress-free temperature of SiC fiber reinforced titanium matrix composites was 700°C based on neutron diffraction. Li *et al*. (2008) ascertained that was 704°C based on the imbalance of the thermal residual strain. In this work, the stress-free temperature used was 700°C.

5. Results and analysis

The radial, axial, hoop residual stress distributions of SiC fiber and titanium alloy matrix were

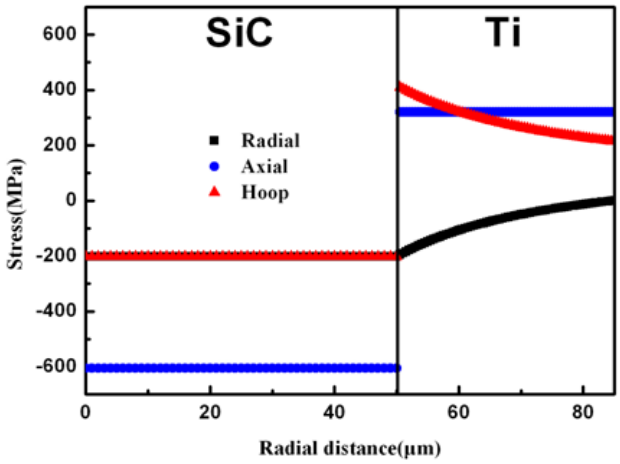

Fig. 3 Residual stress distribution for the titanium matrix composites containing about 35% SiC_f after cooling through 680 K

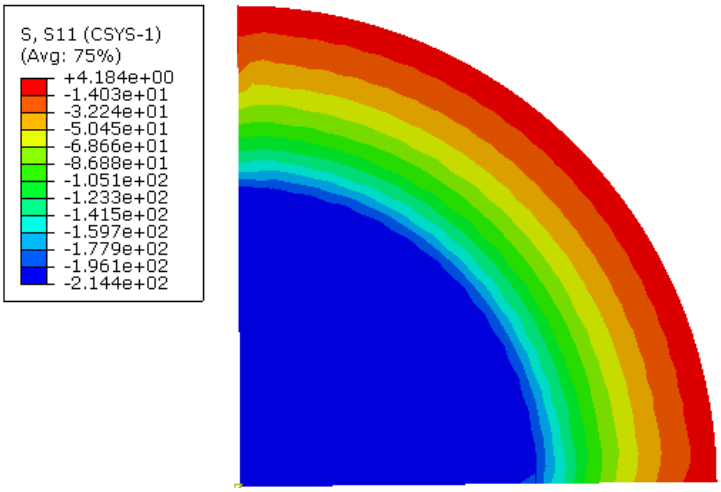

Fig. 4 The radial residual stress nephogram for the titanium matrix composites containing about 35% SiC_f

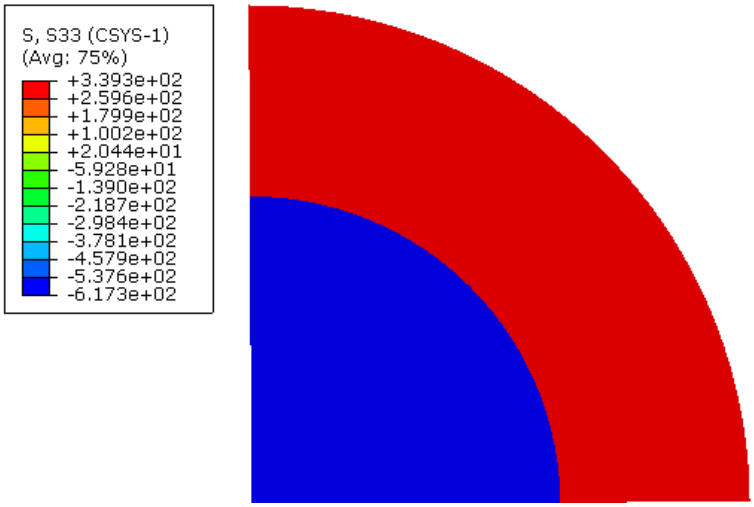

Fig. 5 The axial residual stress nephogram for the titanium matrix composites containing about 35% SiC_f

Table 2 Residual stress in the titanium matrix composites containing about 35% SiC_f after cooling through 680 K

Methods	Radial / MPa	Deviations	Axial / MPa	Deviations
1*	-210	--	-653	--
2	-202	3.8%	-606	7.2%
3	-214	1.9%	-617	5.5%

* 1: Neutron diffraction; 2: Continuous coaxial cylinder model; 3: Finite element model

calculated through the continuous coaxial cylinder model and the finite element software Abaqus, respectively. The results were showed in Figs. 3-5.

As shown in Fig. 3, the radial residual stress in the SiC fiber was compressive stress with the strength of 202 MPa, and the axial residual stress was also compressive stress with the strength of 606 MPa. Seen in Figs. 4-5, both the radial residual stress and axial residual stress was compressive stress with the strength of 214 MPa and 617 MPa, respectively.

Residual stress in the titanium matrix composites containing about 35% SiC_f after cooling through 680 K was obtained by Warrier, S.G. using neutron diffraction. Table 2 showed the comparison between the results obtained through the above two methods and the data reported by Warrier.

As shown in Table 2, deviations between the two theoretical calculation methods and neutron diffraction were all less than 8%. It indicated that both continuous coaxial cylinder model and finite element model were feasible to calculate the residual stress distribution in the continuous SiC fiber reinforced titanium matrix composites.

The main factors which influenced the residual stress in the continuous SiC fiber reinforced titanium matrix composites were: temperature, fiber volume fraction and the coating on SiC fiber, but the temperature was determined by the preparation process. Therefore, the remained two factors were analyzed.

5.1 Fiber volume fraction

The theoretical properties of composites could be obtained by the mixing law, as shown in Eq. (8).

$$X_c = X_{m1}v_{m1} + X_{m2}v_{m2} + \cdots + X_{f1}v_{f1} + X_{f2}v_{f2} + \cdots \tag{8}$$

Where $v_m = \frac{V_m}{V_c}$

X : the proterty of composites, such as elastic modulus, tensile strength;
c : composites;
m : matrix;
f : reinforced phase;
V : volume fration.

As shown in Eq. (8), along with the increment of the SiC fiber volume fraction, the longitudinal property was improved in the titanium matrix composites. But the residual stress in the composites would changed with the change of the SiC fiber volume fraction. So the residual stress was calculated in the axial, hoop, radial direction by using continuous coaxial cylinder model, which was shown in Fig. 6.

As shown in Fig. 6, along with the increment of the SiC fiber volume fraction, the axial, hoop residual stress was increased in the titanium matrix composites, but the radial residual stress was reduced. So, the equivalent residual stress was proposed based on the calculation of equivalent stress(as shown in Eq. (9)).

$$\overline{\sigma} = \frac{1}{\sqrt{2}}\sqrt{(\sigma_x - \sigma_y)^2 + (\sigma_y - \sigma_z)^2 + (\sigma_z - \sigma_x)^2 + 6(\tau_{xy}^2 + \tau_{yz}^2 + \tau_{zx}^2)} \tag{9}$$

The equivalent residual stress in the titanium matrix composites with different fiber volume fractions was calculated, as shown in Fig. 7.

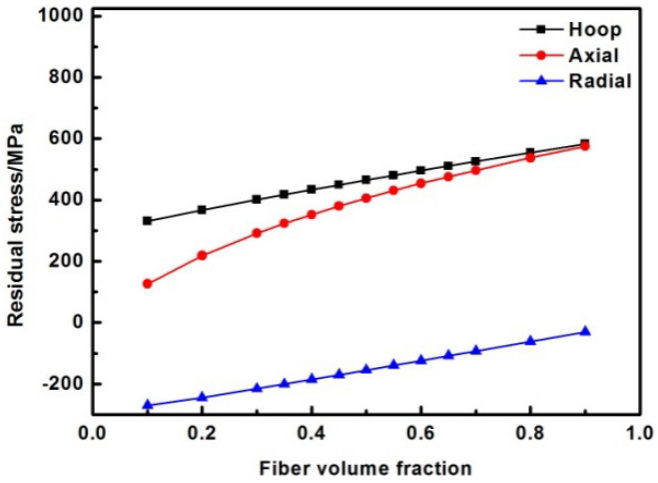

Fig. 6 The residual stress distribution of the composites with different fiber volume fractions

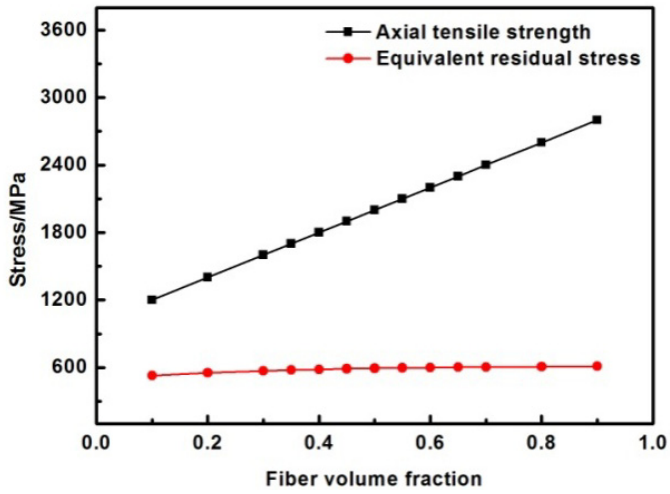

Fig. 7 The equivalent residual stress and axial tensile strength of the composites with different fiber volume fractions

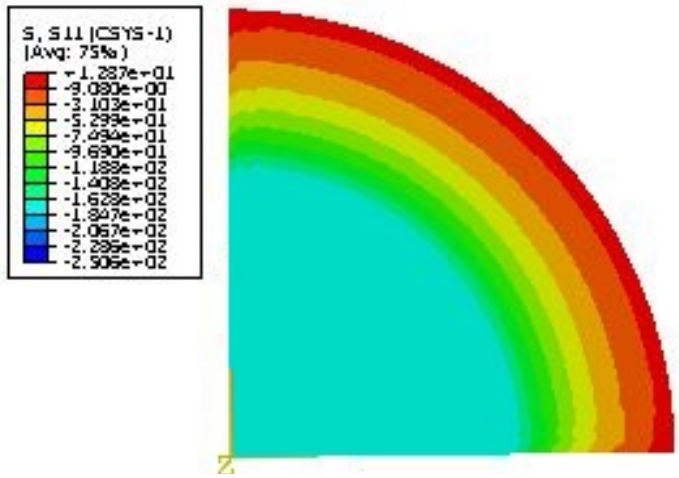

Fig. 8 The radial residual stress nephogram for the SiC fibers with carbon coating reinforced titanium matrix composites

Meanwhile, considering the residual stress, Eq. (10) could be obtained based on the mixing law

$$\sigma_c = (\sigma_m - R_m)v_m + (\sigma_f - R_f)v_f \tag{10}$$

σ : The axial tensile strength;
R : The axial residual stress;
c : composites;
m : titanium matrix;
V : volume fration.

The axial tensile strength of the composites could be calculated based on Eq. (10), as shown in

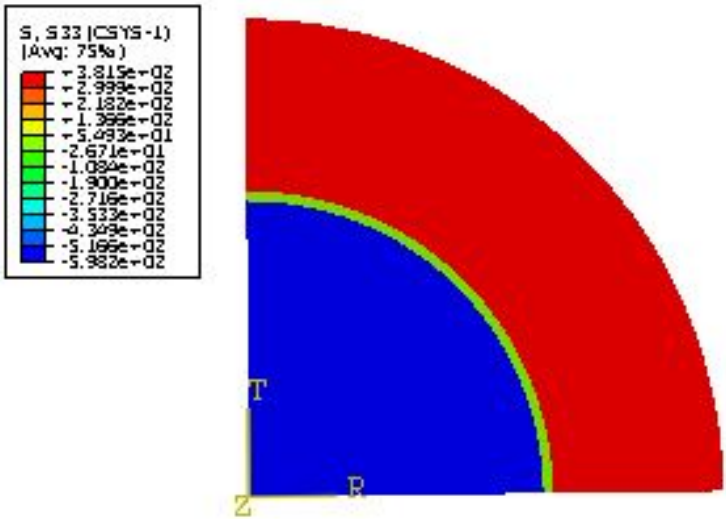

Fig. 9 The axial residual stress nephogram for the SiC fibers with carbon coating reinforced titanium matrix composites

Table 3 The comparison of residual stress in the composites with and without *C* coating

Residual stress	SiC fibers		Titanium matrix	
	Radial / MPa	Axial / MPa	Radial / MPa	Axial / MPa
Without *C* coating	-214	-617	-214	339
With *C* coating	-184	-584	-171	324
Reduction	-14%	-5.3%	-20%	-4.4%

Fig. 7. It was seen in Fig. 7 that along with the increment of the SiC fiber volume fraction, the axial tensile strength was improved, while the equivalent residual stress was not significantly changed, keeping the intensity around 600 MPa. According to the above analysis, considering the residual stress, it was theorized that the longitudinal property in the titanium matrix composites was improved along with the increment of the SiC fiber volume fraction.

5.2 Carbon coating

Figs. 8-9 showed the radial, axial residual stress nephogram for the SiC fibers and titanium matrix when adding a 2 μm thickness carbon coating on the SiC fiber.

According to the above results, the comparison of residual stress in the composites with and without *C* coating was shown in Table 3.

As shown in Table 3, there was a pronounced reduction of the radial residual stress in the titanium matrix composites when there was carbon coating on the surface of the SiC fiber, because carbon coating could effectively reduce the coefficient of thermal expansion mismatch between the fiber and the titanium matrix, meanwhile, the consumption of carbon coating could protect SiC fibers effectively, so as to ensure the high-performance of the composites.

If a new coating on the SiC fiber was designed, it could be evaluated by the two theoretical

calculation methods of thermal residual stress mentioned above. So, the support of design and optimization of composites was provided though the study of this paper.

6. Conclusions

It was feasible to use continuous coaxial cylinder model and finite element model for calculations and analysis of the residual stress in continuous SiC fiber reinforced titanium matrix composites, because the deviations between the theoretical calculation results and the test results were less than 8%. In the titanium matrix composites, along with the increment of the SiC fiber volume fraction, the longitudinal property was improved, while the equivalent residual stress was not significantly changed, keeping the intensity around 600 MPa. There was a pronounced reduction of the radial residual stress in the titanium matrix composites when there was carbon coating on the surface of the SiC fiber, because carbon coating could effectively reduce the coefficient of thermal expansion mismatch between the fiber and the titanium matrix, meanwhile, the consumption of carbon coating could protect SiC fibers effectively, so as to ensure the high-performance of the composites.

Acknowledgments

The research described in this paper was financially supported by National Natural Science Foundation of China under Grant No: 51205376.

References

Arsenault, R.J. and Taya, M. (1987), "Thermal residual stress in metal matrix composite", *Acta Metall*., **35**(3), 651-659.

Feillard, P. (1996), "The high temperature behavior of long fibre reinforced titanium under transverse loading", *Acta Metallurgica*, **44**(2), 643-656.

Fukushima, A., Fujiwara, C., Kagawa, Y. and Masuda, C. (2000), "Effect of interfacial properties on tensile strength in SiC/Ti-15-3 composites", *Mater. Sci. Eng. A*, **276**(1-2), 243-249.

Gundel, D.B. and Wawner, F.E. (1996), "Experimental and theoretical assessment of the longitudinal tensile strength of unidirectional SiC-fiber/titanium-matrix composites", *Compos. Sci. Tech*., **57**(4), 471-481.

Gundel, D.B., Warrier, S.G. and Miracle, D.B. (1999), "The transverse tensile behavior of SiC fiber/Ti-6Al-4V composites: 2. Stress distribution and interface failure", *Compos. Sci. Tech*., **59**(7), 1087-1096.

Huang, B., Yang, Y.Q., Luo, H.J. and Yuan, M.N. (2009), "Effects of the coating system and interfacial region thickness on the thermal residual stresses in SiC_f/Ti-6Al-4V composites", *Mater. Des*., **30**(3), 718-722.

Li, J.K., Yang, Y.Q., Luo, X., Yuan, M.N., Li, L.L. and Zhang, L.W. (2008), "Thermal residual stress in continuous SiC fiber reinforced titanium matrix composites", *Rare Metal Mater. Eng*., **37**(4), 621-624.

Lou, J.H., Yang, Y.Q., Luo, X., Yuan, M.N. and Feng, G.H. (2010), "The analysis on transverse tensile behavior of SiC/Ti-6Al-4V", *Mater. Des*., **31**(8), 3949-3953.

Ma, Z.J., Yang, Y.Q., Zhu, Y. and Chen. Y. (2004), "Effect of fiber distribution on residual thermal stress in titanium matrix composite", *Trans. Nonferrous Met. Soc. China*, **14**(2), 330-334.

Majumdar, B.S. (1999), "Development and characterization of new coatings for improved balance of mechanical properties of titanium matrix composites", *Mater. Sci. Eng. A*, **259**(2), 171-188.

Mao, W.G., Chen, Q., Dai, C.Y., Yang, L., Zhou, Y.C. and Lu, C. (2010), "Effects of piezo-spectroscopic coefficients of 8 wt.% Y_2O_3 stabilized ZrO_2 on residual stress measurement of thermal barrier coatings by Raman spectroscopy", *Surf. Coat. Tech.*, **204**, 3573-3577.

Mikata, Y. and Taya, M. (1985), "Stress field in a coated continuous fiber composite subjected to thermo-mechanical loadings", *J. Compos. Mater.*, **19**(6), 554-578.

Oddershede, J., Schmidt, S., Poulsen, H.F., Sorensen, H.O., Wright, J. and Reimers, W. (2010), "Determining grain resolved in polycrystalline materials using three-dimensional X-ray diffraction", *J. Appl. Crystallogr.*, **43**, 539-549.

Qu, H.T., Ren, X.P., Hou, H.L., Zhao, B. and Li, S.X. (2011), "Interfacial behaviors in SiC fiber reinforced titanium matrix composites during thermal exposure", *Adv. Mater. Res.*, **295-297**, 880-885.

Subramanian, P.R., Krishnamurthy, S., Keller, S.T. and Mendiratta, M.G. (1998), "Processing of continuously reinforced Ti-alloy metal matrix composites(MMC) by magnetron sputtering", *Mater. Sci. Eng. A*, **244**(1), 1-10.

Thomas, M.P. and Winstone, M.R. (1999), "Longitudinal yielding behaviour of SiC-fibre-reinforced titanium-matrix composites", *Compos. Sci. Tech.*, **59**(2), 297-303.

Vassel, A. (1999), "Continuous fibre reinforced titanium and aluminium composites: A comparison", *Mater. Eng. A*, **263**(2), 305-313.

Warrier, S.G., Rangaswamy, P., Bourke, M.A.M. and Krishnamurthy, S. (1999), "Assessment of the fiber/matrix interface bond strength in SiC/Ti-6Al-4V composites", *Mater. Sci. Eng. A*, **259**(2), 220-227.

Warwick, C.M. and Clyne, T.W. (1991), "Development of composite coaxial cylinder stress analysis model and its application to SiC monofilament systems", *J. Mater. Sci.*, **26**(14), 38177-3827.

Woo, W., Em, V., Mikula, P., An, G.B. and Seong, B.S. (2011), "Neutron diffraction measurements of residual stresses in a 50 mm thick weld", *Mater. Sci. Eng. A*, **528**(12), 4120-4124.

Wood, M. and Close, M.W. (1995), "Fibre-reinforced intermetallic compounds by physical vapour deposition", *Mater. Sci. Eng. A*, **192/193**(2), 590-596.

CC